

1  
2  
3  
4 **The Effect of Representing Bromine from VLS on the**  
5 **Simulation and Evolution of Antarctic Ozone**  
6

7  
8 Luke D. Oman<sup>1</sup>, Anne R. Douglass<sup>1</sup>, Ross J. Salawitch<sup>2</sup>,  
9 Timothy P. Canty<sup>2</sup>, Jerald R. Ziemke<sup>1,3</sup>, and Michael Manyin<sup>1,4</sup>

10  
11  
12 <sup>1</sup>*NASA Goddard Space Flight Center, Greenbelt, MD, USA*

13 <sup>2</sup>*University of Maryland, College Park, MD, USA*

14 <sup>3</sup>*Morgan State University, Baltimore, MD, USA*

15 <sup>4</sup>*Science Systems and Applications, Inc., Lanham, MD, USA*  
16  
17

18  
19 Submitted to Geophysical Research Letters  
20  
21  
22  
23  
24  
25

26 Key points:

- 27  
28 1. Including 5 ppt of Br from VLS reduces biases with observed ozone and BrO  
29  
30 2. Resolves a discrepancy with an observational derived parametric model  
31  
32 3. Causes a decade later recovery of Antarctic ozone to 1980 levels  
33  
34  
35

36 *Corresponding Author:*

37 Luke D. Oman

38 NASA Goddard Space Flight Center

39 Atmospheric Chemistry and Dynamics Laboratory

40 Code 614

41 Greenbelt, MD 20771

42 *E-mail:* [luke.d.oman@nasa.gov](mailto:luke.d.oman@nasa.gov)  
43

## 44 **Abstract**

45 We use the Goddard Earth Observing System Chemistry-Climate Model  
46 (GEOSCCM), a contributor to both the 2010 and 2014 WMO Ozone Assessment  
47 Reports, to show that inclusion of 5 parts per trillion (ppt) of stratospheric bromine  
48 ( $\text{Br}_y$ ) from very short-lived substances (VSLS) is responsible for about a decade  
49 delay in ozone hole recovery. These results partially explain the significantly later  
50 recovery of Antarctic ozone noted in the 2014 report, as bromine from VSLS was not  
51 included in the 2010 Assessment. We show multiple lines of evidence that  
52 simulations that account for VSLS  $\text{Br}_y$  are in better agreement with both total  
53 column  $\text{BrO}$  and the seasonal evolution of Antarctic ozone reported by the Ozone  
54 Monitoring Instrument (OMI) on NASA's Aura satellite. In addition, the near zero  
55 ozone levels observed in the deep Antarctic lower stratospheric polar vortex are  
56 only reproduced in a simulation that includes this  $\text{Br}_y$  source from VSLS.

## 57 **1. Introduction**

58 Simulations of the future evolution of the ozone layer show that the time  
59 frame of ozone recovery depends on the halogen and greenhouse gas (GHG)  
60 emissions scenarios and forecast changes in the temperature and circulation of the  
61 stratosphere, each with varying importance dependent on latitude and season  
62 [Eyring *et al.*, 2013a; Oman *et al.*, 2014; World Meteorological Organization (WMO),  
63 2014]. Bromine plays an integral part in determining the atmospheric abundance of  
64 ozone and its effectiveness per molecule at destroying ozone is approximately 45-65  
65 times greater than chlorine [Daniel *et al.*, 1999; Sinnhuber *et al.*, 2009]. In addition,  
66 the bromine impact on ozone depletion is larger with higher chlorine [McElroy *et al.*,

67 1986] as well as with enhanced sulfate aerosol loading, like following large volcanic  
68 eruptions [Salawitch et al., 2005].

69 Bromine from very short-lived substances (VSLS), mainly bromoform  
70 (CHBr<sub>3</sub>) and dibromomethane (CH<sub>2</sub>Br<sub>2</sub>) has also been shown to be an important  
71 part of the total atmospheric burden of bromine and ozone layer chemistry [Ko et  
72 al., 1997; Sturges et al., 2000; Salawitch et al., 2005]. Theys et al. [2007] estimated  
73 that VSLS supply 6 to 8 parts per trillion (ppt) of stratospheric Br<sub>y</sub> based on  
74 retrieval of stratospheric and tropospheric column BrO at Reunion-Island (20.9°S).  
75 Salawitch et al. [2010], focusing on the Arctic, found that 5 to 10 ppt of stratospheric  
76 bromine from VSLS is needed to achieve consistency with aircraft and satellite  
77 measurements of BrO. Liang et al. [2014] quantified the chemical and physical  
78 transformations of VSLS after release into the marine boundary layer using the  
79 Goddard Earth Observing System Chemistry-Climate Model (GEOSCCM) and  
80 concluded VSLS supply about 8 ppt of bromine to the base of the tropical  
81 tropopause layer. Measurements of upper stratospheric BrO from the Microwave  
82 Limb Sounder (MLS), balloon-borne DOAS (Differential Optical Absorption  
83 Spectroscopy), and the Scanning Imaging Absorption Spectrometer for Atmospheric  
84 Cartography (SCIAMACHY) yield estimates for VSLS supply of stratospheric Br<sub>y</sub> of  
85  $5 \pm 4.5$  ppt [Millan et al., 2012],  $5.2 \pm 2.5$  ppt [Dorf et al., 2008], and  $7 \pm 6$  ppt  
86 [Parrella et al., 2013], respectively.

87 A few studies examined the impact of this additional bromine on  
88 stratospheric ozone concentrations. Frieler et al. [2006] showed inclusion of  
89 bromine from VSLS led to better agreement between observed and modeled loss of

90 Arctic ozone for a particular winter. *Feng et al.* [2007], focusing on midlatitude  
91 ozone, found a 10 DU decrease by including 5 ppt of bromine from VLSL. *Yang et al.*  
92 [2014] made a rough estimate of 6-8 years later recovery of the Antarctic ozone hole  
93 due to 5 ppt of bromine from VLSL based on time-slice experiments with various  
94 chlorine and bromine levels. *Sinnhuber and Meul* [2015] found closer agreement in a  
95 simulation with the chemistry climate model (CCM) EMAC to observed trends of  
96 global column ozone when including bromine from VLSL.

97 An outstanding issue has been the difference in Antarctic ozone recovery  
98 projections obtained using CCMs and projections derived from observations.  
99 *Newman et al.* [2006] used an observationally derived parametric model of ozone  
100 hole area to predict recovery of Antarctic ozone to 1980 levels around 2068 under  
101 the Ab halogen scenario [*WMO*, 2003]. CCMs used in the WMO 2010 Assessment  
102 [*WMO*, 2011] returned Antarctic column ozone to 1980 levels by 2051 on average,  
103 much earlier than forecast by the parametric model. The scientific summary  
104 suggested that failure of the parametric model to account for an upper stratospheric  
105 ozone increase, which would be caused by GHG-induced changes in circulation and  
106 temperature, could explain this difference [*WMO*, 2011]. However, *Eyring et al.*  
107 [2010] found only a small difference in October Antarctic ozone values for  
108 simulations using various GHG scenarios.

109           Significantly later recovery of October Antarctic ozone was noted in Chapter  
110 3 of the 2014 WMO Ozone Assessment [*WMO*, 2014] by each of the four models  
111 (CMAM, GEOSCCM, UMSLIMCAT, WACCM) that contributed simulations for this  
112 most recent Assessment, compared to results from a larger number of models that

113 contributed to the 2010 Assessment [WMO, 2011]. However, they were unable to  
114 explain the cause of the later recovery, given the model simulations available at the  
115 time. The multi-model mean of these latest simulations indicated that return of  
116 Antarctic O<sub>3</sub> to 1980 levels would not occur until after 2080. Small differences in the  
117 base ozone depleting substance (ODS) scenario relative to that used in the prior  
118 Assessment [Velders and Daniel, 2014] caused a small 3-4% increase in vortex Cl<sub>y</sub> in  
119 the later half of the 21<sup>st</sup> century for the updated simulations [Oman and Douglass,  
120 2014] and do not explain the later recovery. However, all of the new simulations  
121 represented the impact of VSLS on stratospheric Br<sub>y</sub> in the form of a constant, extra  
122 5 ppt of bromine (note: VSLS bromine is independent of ODS specifications, since  
123 the VSLS are biogenic and not anthropogenic). The impact of VSLS-based Br<sub>y</sub> on  
124 ozone recovery was not simulated in the 2010 Assessment.

125         Here we use the GEOSCCM, which contributed to both the 2010 and 2014  
126 WMO Assessments, to quantify the effect of an additional 5 ppt of stratospheric  
127 bromine from VSLS on both the recovery of the ozone layer over the 21<sup>st</sup> century  
128 and the current seasonal evolution of the Antarctic ozone hole. We use 5 ppt for  
129 VSLS bromine because this is the best estimate given by WMO [2014]. We show that  
130 inclusion of bromine from VSLS partly explains why the 2014 Assessment reported  
131 a significant delay in the recovery of the Antarctic ozone layer. Section 2 describes  
132 the model and forcing scenarios as well as the measurements used to evaluate the  
133 effect of this additional bromine. Results of these simulations and conclusions  
134 follow.

135

## 136 2. Model, Forcing Scenarios, and Observations

137 The GEOSCCM coupled to the stratospheric chemistry module, StratChem  
138 [Pawson *et al.*, 2008; Oman and Douglass, 2014], was used to quantify the impact of  
139 including VSLs bromine on the ozone layer, focusing on the effects over Antarctica.  
140 The model was run at  $2^\circ \times 2.5^\circ$  (lat.  $\times$  long.) horizontal resolution with 72 vertical  
141 layers from the surface up to 80 km, with photochemical input data from JPL 2010  
142 [Sander *et al.*, 2011]. Evaluation of GEOSCCM using process-oriented diagnostics  
143 was conducted in both CCMVal-1 [Eyring *et al.*, 2006] and CCMVal-2 [SPARC CCMVal  
144 2010]. GEOSCCM performed well in both chemical and transport related processes  
145 [SPARC CCMVal 2010; Strahan *et al.*, 2011; Douglass *et al.*, 2012] and some  
146 additional improvements were reported in Oman and Douglass [2014].

147 Both GEOSCCM simulations described here used GHG concentrations from the  
148 Representative Concentration Pathway (RCP) 6.0, which produces  $6.0 \text{ W/m}^2$   
149 anthropogenic radiative forcing of climate by 2100 [Meinshausen *et al.*, 2011; Moss  
150 *et al.*, 2010]. Both used the A1 2014 scenario for ODS [Velders and Daniel, 2014], the  
151 same as used in the 2014 WMO Assessment [WMO, 2014]. The first of these, the  
152 control simulation (A12014\_0Br), does not include any  $\text{Br}_y$  from VSLs, as assumed  
153 for the 2010 WMO [WMO, 2011] and earlier Assessments. The second simulation  
154 (A12014\_5Br) includes an extra 5 ppt of  $\text{CH}_3\text{Br}$  to represent VSLs, as recommended  
155 by the Chemistry Climate Modeling Initiative (CCMI) [Eyring *et al.*, 2013b].

156 Sea surface temperature and sea ice concentrations were prescribed from a  
157 simulation using the Community Earth System Model version 1 (CESM1) conducted  
158 from 1960-2099 [Gent *et al.*, 2011], forced with the same RCP 6.0 GHG scenario.

159 Observations from the Ozone Monitoring Instrument (OMI) and Microwave Limb  
160 Sounder (MLS) on the NASA Aura satellite are used to evaluate the simulation of  
161 ozone and bromine monoxide (BrO) from Jan. 2005 to Dec. 2015. OMI level-3  
162 gridded daily total column ozone values are determined using the OMT03 version  
163 8.5 retrieval algorithm (*Bhartia, 2007*). In addition, vertical daily ozone  
164 measurements from MLS level-2 version 4.2 [*Livesey et al., 2015*] were used in the  
165 evaluation. Description and access to these satellite data records is at  
166 <http://disc.sci.gsfc.nasa.gov/Aura> .

167 For the comparison of modeled and measured BrO, model output is sampled  
168 at the locations for which OMI measurements are available. Due to the diel cycle of  
169 BrO, model output was sampling at 2 p.m. local solar time, close to the time of OMI  
170 overpass. Version 3 retrievals of total column BrO from OMI were used for  
171 comparison with the GEOSCCM output; data and description are at  
172 [http://disc.sci.gsfc.nasa.gov/Aura/data-holdings/OMI/ombro\\_v003.shtml](http://disc.sci.gsfc.nasa.gov/Aura/data-holdings/OMI/ombro_v003.shtml) .  
173 Destriped, level-2 total column observations (OMBRO.003) and  $1\sigma$  uncertainties  
174 (based on spectral fitting) were filtered using flags “xtrackqualityflag” to account for  
175 the OMI row anomaly and “maindataqualityflag” to remove invalid data. The  
176 filtered data were then gridded to match the latitudes and longitudes of the  
177 GEOSCCM simulations. Daily, gridded satellite observations of total column BrO and  
178 the associated uncertainty were cosine weighted and averaged between 60 to 90°S.  
179 Similarly, GEOSCCM output at 2 p.m. was weighted and averaged, but only for those  
180 model grid points where corresponding observations were available. Finally, time  
181 series of seasonal averages (JJA) were generated for modeled total column BrO, as

182 well as for satellite observation and uncertainty of total column BrO.

183

### 184 **3. Results/ Discussion**

185 Here, we show that inclusion of 5 ppt of CH<sub>3</sub>Br to represent the bromine from  
186 VLSL impacts both the present seasonal evolution of the Antarctic ozone layer and  
187 its recovery over the 21<sup>st</sup> century. The simulated present day seasonal cycle of  
188 ozone over Antarctica compares better with OMI total column ozone measurements  
189 when the VLSL contribution is included. Figure 1 shows the daily average total  
190 column ozone (DU) amounts from 60-90°S for the A12014\_5Br (blue curve) and  
191 A12014\_0Br (red curve) simulations and from OMI observations (black curve), with  
192 both observations and simulations averaged over 2005-2015. The additional  
193 bromine decreases ozone between 6-20 DU, with the largest decline occurring in  
194 September. The faster onset of the ozone hole formation and the minimum ozone  
195 amounts, around 1 October are in better agreement with observation than found  
196 using the simulation without VLSL bromine. GEOSCCM does have a somewhat  
197 delayed breakup of the polar vortex, which is seen in the slower ozone increase  
198 during November and December.

199 It is well known that ozone deep in the Antarctic polar vortex between 14-18  
200 km drops to near zero levels, typically in the last week of September and the first  
201 week of October [*Hofmann et al., 1997*]. Figure 2 shows the daily ozone partial  
202 pressure (millipascals) at 80°S for the simulations A12014\_5Br and A12014\_0Br,  
203 and MLS ozone from 1 September to 30 October, all averaged over 2005-2009. The  
204 simulation including VLSL bromine is much closer to the very low abundance of



205 ozone observed from MLS and the South Pole ozonesonde record in the lower  
206 stratosphere, with the near zero values routinely reached during the mid-late 1990s  
207 and early 2000s. These near zero values are not seen the A12014\_0Br simulation.  
208 The ozone profile difference (%) between these two simulations and MLS  
209 observations over 60 to 82°S, for a few select days surrounding the ozone minimum,  
210 is shown in Figure S1. This comparison also shows improved agreement between  
211 pressures of 200 to 10 hPa when the VSLs source of 5 ppt of bromine is included.

212       October average Antarctic total column ozone is the commonly used measure  
213 of ozone depletion and recovery in WMO Ozone Assessments and the SPARC  
214 CCMVal-2 Report (*SPARC CCMVal*, 2010). Figure 3 shows the October average total  
215 column ozone (DU) over 60-90°S from 1960-2099 for our two simulations. The  
216 A12014\_5Br simulation shows almost a decade later recovery of Antarctic polar  
217 ozone to 1980 levels. As expected, the largest ozone differences between these two  
218 simulations occur when chlorine loading levels are within 50% of the maximum.  
219 GEOSCCM October total column ozone returns to 1980 levels by approximately  
220 2062 in the A12014\_0Br simulation and around 2071 in the A12014\_5Br simulation.  
221 These simulations represent a pair of runs, the difference between these two  
222 simulations could be amplified or damped by natural internal variability. However,  
223 the recovery date is also delayed by over a decade for the four models that included  
224 VSLs bromine for the 2014 assessment but not for 2010. Therefore, we expect that  
225 the significant difference between our pair of simulations would persist over  
226 multiple ensemble members. This later recovery date is now similar to the estimate  
227 from a parametric model [*Newman et al.*, 2006] using available data at the time and

228 resolves a discrepancy between it and recovery estimates from previous WMO  
229 Assessments [2011].

230 Comparisons of total column BrO retrieved from the OMI instrument with  
231 simulated BrO columns supports inclusion of a contribution of VSLs, similar to  
232 results obtained by *Salawitch et al.* [2010] and *Liang et al.* [2014]. Figure S2 shows  
233 total column BrO from OMI averaged over the months of June to August, for 60 to  
234 90°S, for the years 2005 to 2015 compared to GEOSCCM simulations for the same  
235 months, latitude range, and year. Inclusion of the extra 5 ppt of bromine reduces,  
236 but does not completely eliminate, a systematic low bias between simulated and  
237 observed column BrO. Enhanced tropospheric BrO from surface release is not  
238 included in our GEOSCCM simulations, which could account for the low bias in  
239 modeled BrO. *Roscoe et al.* [2014] show surface release of bromine typically  
240 contributes between 1 and  $3 \times 10^{13}$  mol cm<sup>-2</sup> of tropospheric BrO, distributed  
241 throughout the free troposphere, at Halley Bay (75.6°S). Another possibility for the  
242 underestimate of column BrO could be model misrepresentation of the BrO/Br<sub>y</sub> in  
243 the troposphere. On the other hand, the actual contribution from VSLs to  
244 stratospheric Br<sub>y</sub> could be larger than 5 ppt. The results presented in Figure S2 are  
245 consistent with estimates of at least 5 ppt of bromine being supplied by VSLs  
246 [*Salawitch et al.*, 2005; *Dorf et al.*, 2008; *Theys et al.*, 2007; *Salawitch et al.*, 2010;  
247 *Parrella et al.*, 2013, *Liang et al.*, 2014].

248 Time series of BrO, BrCl, and OClO at 50 hPa from the two GEOSCCM  
249 simulations, averaged over 60-90°S during Aug.-Oct are shown in Figure S3. Neither  
250 BrO, BrCl, nor OClO return to their respective 1980 levels by the end of the

251 simulations. The time series of OClO behaves in a similar manner to BrO and BrCl  
252 because the abundance of OClO in the polar vortex is much more sensitive to BrO  
253 than ClO [Salawitch *et al.*, 1988]. The difference between the two simulations grows  
254 larger with time, reflecting a much larger role for ozone loss due to the BrO+ClO  
255 cycle in A12014\_5Br than the A12014\_0Br simulation during the latter part of this  
256 century. Together, Figures 3, S2, and S3 show that including all the sources of  
257 stratospheric bromine causes about a decade delay in the recovery of the Antarctic  
258 ozone hole.

259 Including supply of stratospheric bromine from VLS reduces ozone columns  
260 nearly everywhere in the model, with the smallest changes in the tropics and the  
261 largest decreases over the high latitudes during spring (Figure 4). The effect of this  
262 extra bromine is largest during the time period of peak chlorine (1990 – 2019). For  
263 this three-decade period, inclusion of Br<sub>v</sub> from VLS decreases total column ozone  
264 by 16-22 DU over Antarctica during September. In the Northern Hemisphere high  
265 latitudes, ozone is reduced by 10-20 DU during March. The tropical total column  
266 ozone decrease is typically less than 2 DU. This three-decade time period also  
267 includes the eruption of Mt. Pinatubo in June 1991, shortly after which ozone loss  
268 due to bromine was larger in the A1204\_5Br simulation. However, the enhanced  
269 ozone loss following the eruption of Mt Pinatubo follows the aerosol lifetime in the  
270 stratosphere of 1-3 years and does not significantly impact the 30-year average  
271 response.

272

#### 273 **4. Conclusions**

274 Inclusion of 5 ppt of stratospheric bromine to represent VSLS in GEOSCCM  
275 results in better agreement with OMI measurement of total column BrO and causes  
276 several important changes in the simulation of the seasonal evolution and recovery  
277 over the 21<sup>st</sup> century of Antarctic ozone. A high bias in simulated SH polar total  
278 column ozone with respect to OMI observations collected over 2005 to 2015 is  
279 significantly reduced. Including VSLS bromine causes the minimum seasonal ozone  
280 column to occur about a week earlier, in closer agreement with OMI observations.  
281 The very low to near zero ozone concentrations observed in the deep Antarctic  
282 lower stratospheric polar vortex during late September into early October during  
283 the mid-late 1990s and into the early 2000s are only simulated when the VSLS  
284 bromine source is included.

285 According to our GEOSCCM simulations, recovery of Antarctic ozone is  
286 delayed by about a decade upon including the VSLS contribution to stratospheric  
287 bromine. October Antarctic ozone columns are projected to return to 1980 levels  
288 around 2071, in close agreement with a recovery year of 2068 based on an  
289 empirical, parametric model [Newman *et al.*, 2006]. The 2010 WMO Assessment  
290 [WMO, 2011] attributed an earlier recovery year of ~2051, provided by simulations  
291 from 17 CCMs, to meteorological and dynamical effects of GHGs on Antarctic ozone  
292 that were not considered in the parametric model. However, most of the CCM  
293 simulations used in WMO [2011] neglected VSLS bromine and WMO [2014] showed  
294 the meteorological and dynamical effects of GHGs on Antarctic ozone recovery was  
295 small. These results show that a constant addition of 5 ppt of bromine cause almost  
296 a decade later recovery of Antarctic ozone and suggest that any future growth or

297 new emissions of bromine containing compounds, as low as a couple ppt, could  
298 significantly impact the projected ozone recovery date. Our study also suggests  
299 models estimates of polar ozone recovery for the next Assessment should include a  
300 realistic treatment of the VSLs contribution to stratospheric bromine. If bromine  
301 from VSLs are neglected, recovery dates will be biased early by perhaps as much as  
302 a decade.

303

#### 304 **Acknowledgements**

305 We thank the NASA ACMAP, Aura, and MAP program for supporting this  
306 research. We would like to thank two anonymous reviewers for their helpful  
307 comments and suggestion to improve this manuscript. We also thank those involved  
308 in model development at GSFC, and high-performance computing resources  
309 provided by NASA's Advanced Supercomputing (NAS) Division and the NASA Center  
310 for Climate Simulation (NCCS). All data and model output used in these figures will  
311 be available with the link to this publication at the GEOSCCM website (<http://acd-ext.gsfc.nasa.gov/Projects/GEOSCCM/>), additional information is available by  
312 contacting the corresponding author ([luke.d.oman@nasa.gov](mailto:luke.d.oman@nasa.gov)).

314

#### 315 **References**

316 Bhartia, P. K. (2007), Total ozone from backscattered ultraviolet measurements, in:  
317 Observing Systems for Atmospheric Composition, L'Aquila, Italy, 20-24  
318 September, 2004, edited by: Visconti, G., Di Carlo, P., Brune, W., Schoeberl, W.,  
319 and Wahner, A., Springer, 48-63.

320 Daniel, J. S., S. Solomon, R. W. Portmann, and R. R. Garcia (1999), Stratospheric  
321 ozone destruction: The importance of bromine relative to chlorine, *J. Geophys.*  
322 *Res.*, 104, 23871–23880.

323 Dorf, M., A. Butz, C. Camy-Peyre, M. P. Chipperfield, L. Kritten, and K. Pfeilsticker  
324 (2008), Bromine in the tropical troposphere and stratosphere as derived from  
325 balloon-borne BrO observations, *Atmos. Chem. Phys.*, 8, 7265–7271,  
326 doi:10.5194/acp-8-7265-2008.

327 Douglass, A. R., R. S. Stolarski, S. E. Strahan, and L. D. Oman (2012), Understanding  
328 differences in upper stratospheric ozone response to changes in chlorine and  
329 temperature as computed using CCMVal-2 models, *J. Geophys. Res.*, 117, D16306,  
330 doi:10.1029/2012JD017483.

331 Eyring, V., N. Butchart, D. W. Waugh, H. Akiyoshi, J. Austin, S. Bekki, G. E. Bodeker, B.  
332 A. Boville, C. Brühl, M. P. Chipperfield, E. Cordero, M. Dameris, M. Deushi, V. E.  
333 Fioletov, S. M. Frith, R. R. Garcia, A. Gettelman, M. A. Giorgetta, V. Grewe, L.  
334 Jourdain, D. E. Kinnison, E. Mancini, E. Manzini, M. Marchand, D. R. Marsh, T.  
335 Nagashima, P. A. Newman, J. E. Nielsen, S. Pawson, G. Pitari, D. A. Plummer, E.  
336 Rozanov, M. Schraner, T. G. Shepherd, K. Shibata, R. S. Stolarski, H. Struthers, W.  
337 Tian, and M. Yoshiki (2006), Assessment of temperature, trace species and ozone  
338 in chemistry-climate model simulations of the recent past, *J. Geophys. Res.*, 111,  
339 D22308, doi:10.1029/2006JD007327.

340 Eyring, V., et al. (2010), Sensitivity of 21st century stratospheric ozone to  
341 greenhouse gas scenarios, *Geophys. Res. Lett.*, 37(16), L16807.

342 Eyring, V., et al. (2013a), Long-term ozone changes and associated climate impacts

343 in CMIP5 simulations, *J. Geophys. Res. Atmos.*, 118, 5029–5060,  
344 doi:10.1002/jgrd.50316.

345 Eyring, V., et al. (2013b), Overview of IGAC/SPARC Chemistry-Climate Model  
346 Initiative (CCMI) Community Simulations in Support of Upcoming Ozone and  
347 Climate Assessments, *SPARC Newsletter No. 40*, p. 48-66.

348 Feng, W., M. P. Chipperfield, M. Dorf, K. Pfeilsticker, and P. Ricaud (2007), Mid-  
349 latitude ozone changes: studies with a 3-D CTM forced by ERA-40 analyses,  
350 *Atmos. Chem. Phys.*, 7, 2357–2369, doi:10.5194/acp-7-2357-2007.

351 Frieler, K., M. Rex, R. J. Salawitch, T. Canty, M. Streibel, R. M. Stimpfle, K. Pfeilsticker,  
352 M. Dorf, D. K. Weisenstein, and S. Godin-Beekmann (2006), Toward a better  
353 quantitative understanding of polar stratospheric ozone loss, *Geophys. Res. Lett.*,  
354 33, L10812, doi:10.1029/2005GL025466.

355 Gent, P. R., G. Danabasoglu, L. J. Donner, M. M. Holland, E. C. Hunke, S. R. Jayne, D. M.  
356 Lawrence, et al. (2011), The Community Climate System Model Version 4, *J. Clim.*,  
357 24(19), pp. 4973–4991, doi: 10.1175/2011JCLI4083.

358 Hofmann, D. J., S. J. Oltmans, J. M. Harris, B. J. Johnson, and J. A. Lathrop (1997), Ten  
359 years of ozonesonde measurements at the south pole: Implications for recovery  
360 of springtime Antarctic ozone, *J. Geophys. Res.*, 102(D7), 8931–8943,  
361 doi:10.1029/96JD03749.

362 Ko, M. K. W., N.-D. Sze, C. J. Scott, and D. K. Weisenstein (1997), On the relation  
363 between stratospheric chlorine/bromine loading and short-lived tropospheric  
364 source gases, *J. Geophys. Res.*, 102, 25,507–25,517.

365 Liang, Q., E. Atlas, D. R. Blake, M. Dorf, K. Pfeilsticker, and S. Schauffler (2014),

366 Convective transport of very-short-lived bromocarbons to the stratosphere,  
367 *Atmos. Chem. Phys.*, 14, 5781-5792.

368 Livesey, N. J., W. G. Read, P. A. Wagner, L. Froidevaux, A. Lambert, G. L. Manney, L. F.  
369 Millán-Valle, H. C. Pumphrey, M. L. Santee, M. J. Schwartz, S. Wang, R. A. Fuller, R.  
370 F. Jarnot, B. W. Knosp, and E. Martinez (2015), Version 4.2x Level 2 data quality  
371 and description document, Tech. Rep. JPL D-33509, NASA Jet Propulsion  
372 Laboratory, version 4.2x-1.0.

373 McElroy, M. B., R. J. Salawitch, S.C. Wofsy, and J.A. Logan (1986), Reductions of  
374 Antarctic ozone due to synergistic interactions of chlorine and bromine. *Nature*.  
375 321:759-762.

376 McPeters, R. D., S. Frith, and G. J. Labow (2015), OMI total column ozone: extending  
377 the long-term data record, *Atmos. Meas. Tech.*, 8, 4845–4850, doi:10.5194/amt-  
378 8-4845-2015.

379 Meinshausen, M., et al. (2011), The RCP greenhouse gas concentrations and their  
380 extensions from 1765 to 2300, *Clim. Chang.*, 109(1–2), 213–241.

381 Millan, L., N.J. Livesey, L. Froidevaux, D. Kinnison, R. Harwood, I.A. MacKenzie, and  
382 M.P. Chipperfield (2012), New Aura Microwave Limb Sounder observations of  
383 BrO and implications for Br<sub>y</sub>, *Atmospheric Measurement Techniques*,  
384 doi:10.5194/amt-5-1741-2012.

385 Moss, R. H., et al. (2010), The next generation of scenarios for climate change  
386 research and assessment, *Nature*, 463(7282), 747–756.



387 Oman, L. D., and A. R. Douglass (2014), Improvements in Total Column Ozone in  
388 GEOSCCM and Comparisons with a New Ozone Depleting Substances Scenario, *J.*  
389 *Geophys. Res.*, 119, 5613-5624, doi:10.1002/2014JD021590.

390 Newman, P. A., E. R. Nash, S. R. Kawa, S. A. Montzka, and S. M. Schauffler (2006),  
391 When will the Antarctic ozone hole recover? *Geophys. Res. Lett.*, 33, L12814,  
392 doi:10.1029/2005GL025232.

393 Parrella, J. P., K. Chance, R. J. Salawitch, T. Canty, M. Dorf, and K. Pfeilsticker (2013),  
394 New retrieval of BrO from SCIAMACHY limb: an estimate of the stratospheric  
395 bromine loading during April 2008, *Atmos. Meas. Tech.*, 6, 2549–2561,  
396 doi:10.5194/amt-6-2549-2013.

397 Pawson, S., R. S. Stolarski, A. R. Douglass, P. A. Newman, J. E. Nielsen, S. M. Frith, and  
398 M. L. Gupta (2008), Goddard Earth Observing System chemistry-climate model  
399 simulations of stratospheric ozone-temperature coupling between 1950 and  
400 2005, *J. Geophys. Res.*, 113, D12103, doi:10.1029/2007JD009511.

401 Roscoe, H. K., N. Brough, A. E. Jones, F. Wittrock, A. Richter, M. Van Roozendaal, and  
402 F. Hendrick (2014), Characterisation of vertical BrO distribution during events of  
403 enhanced tropospheric BrO in Antarctica, from combined remote and in-situ  
404 measurements, *J. Quant. Spectrosc. Radiat. Transfer*, 138, 70–81.

405 Salawitch, R. J., S. C. Wofsy, M. B. McElroy (1988), Chemistry of OCIO in the Antarctic  
406 stratosphere: implications for bromine, *Planet. Space Sci.*, 36, 213-224.

407 Salawitch, R. J., D. K. Weisenstein, L. J. Kovalenko, C. E. Sioris, P. O. Wennberg, K.  
408 Chance, M. K. W. Ko, and C. A. McLinden (2005), Sensitivity of ozone to bromine  
409 in the lower stratosphere, *Geophys. Res. Lett.*, 32, L05811,

410 doi:10.1029/2004GL021504.

411 Salawitch, R. J., et al. (2010), A new interpretation of total column BrO during Arctic  
412 spring, *Geophys. Res. Lett.*, 37, L21805, doi:10.1029/2010GL043798.

413 Sander, S. P., J. Abbatt, J. R. Barker, J. B. Burkholder, R. R. Friedl, D. M. Golden, R. E.  
414 Huie, C. E. Kolb, M. J. Kurylo, G. K. Moortgat, V. L. Orkin and P. H. Wine (2011),  
415 Chemical Kinetics and Photochemical Data for Use in Atmospheric Studies,  
416 Evaluation No. 17, JPL Publication 10-6, Jet Propulsion Laboratory, Pasadena.

417 Sinnhuber, B.-M., N. Sheode, M. Sinnhuber, M. P. Chipperfield, and W. Feng (2009),  
418 The contribution of anthropogenic bromine emissions to past stratospheric  
419 ozone trends: A modelling study, *Atmos. Chem. Phys.*, 9, 2863–2871.

420 Sinnhuber, B.-M., and S. Meul (2015), Simulating the impact of emissions of  
421 brominated very short lived substances on past stratospheric ozone trends,  
422 *Geophys. Res. Lett.*, 42, 2449–2456, doi:10.1002/2014GL062975.

423 SPARC CCMVal, SPARC CCMVal Report on the Evaluation of Chemistry-Climate  
424 Models (2010), V. Eyring, T. G. Shepherd, D. W. Waugh (Eds.), SPARC Report No.  
425 5, WCRP-132, WMO/TD-No. 1526,  
426 <http://www.atmosph.physics.utoronto.ca/SPARC>.

427 Strahan, S.E., A.R. Douglass, R.S. Stolarski, and et al. (2011), Using transport  
428 diagnostics to understand chemistry climate model ozone simulations *J. Geophys.*  
429 *Res.*, 116. doi:10.1029/2010JD015360.

430 Sturges, W. T., D. E. Oram, L. J. Carpenter, S. A. Penkett, and A. Engel (2000),  
431 Bromoform as a source of stratospheric Br<sub>y</sub>, *Geophys. Res. Lett.*, 27, 2081-2084.

432 Theys, N., M. Van Roozendael, F. Hendrick, C. Fayt, C. Hermans, J.-L. Baray, F. Goutail,  
433 J.-P. Pommereau, and M. De Maziere (2007), Retrieval of stratospheric and  
434 tropospheric BrO columns from multi-axis DOAS measurements at Reunion  
435 Island (21°S, 56°E), *Atmos. Chem. Phys.*, 7, 4733–4749, doi:10.5194/acp-7-4733-  
436 2007.

437 Velders, G. J. M. and J. S. Daniel (2014), Uncertainty analysis of projections of ozone-  
438 depleting substances: mixing ratios, EESC, ODPs, and GWPs, *Atmos. Chem. Phys.*,  
439 14, 2757-2776, doi:10.5194/acp-14-2757-2014.

440 World Meteorological Organization (2003), Scientific assessment of ozone  
441 depletion: 2002, Global Ozone Research and Monitoring Project-Report No. 47,  
442 498 pp., Geneva, Switzerland.

443 World Meteorological Organization (2011), Scientific assessment of ozone  
444 depletion: 2010, Global Ozone Research and Monitoring Project-Report No. 52,  
445 516 pp., Geneva, Switzerland.

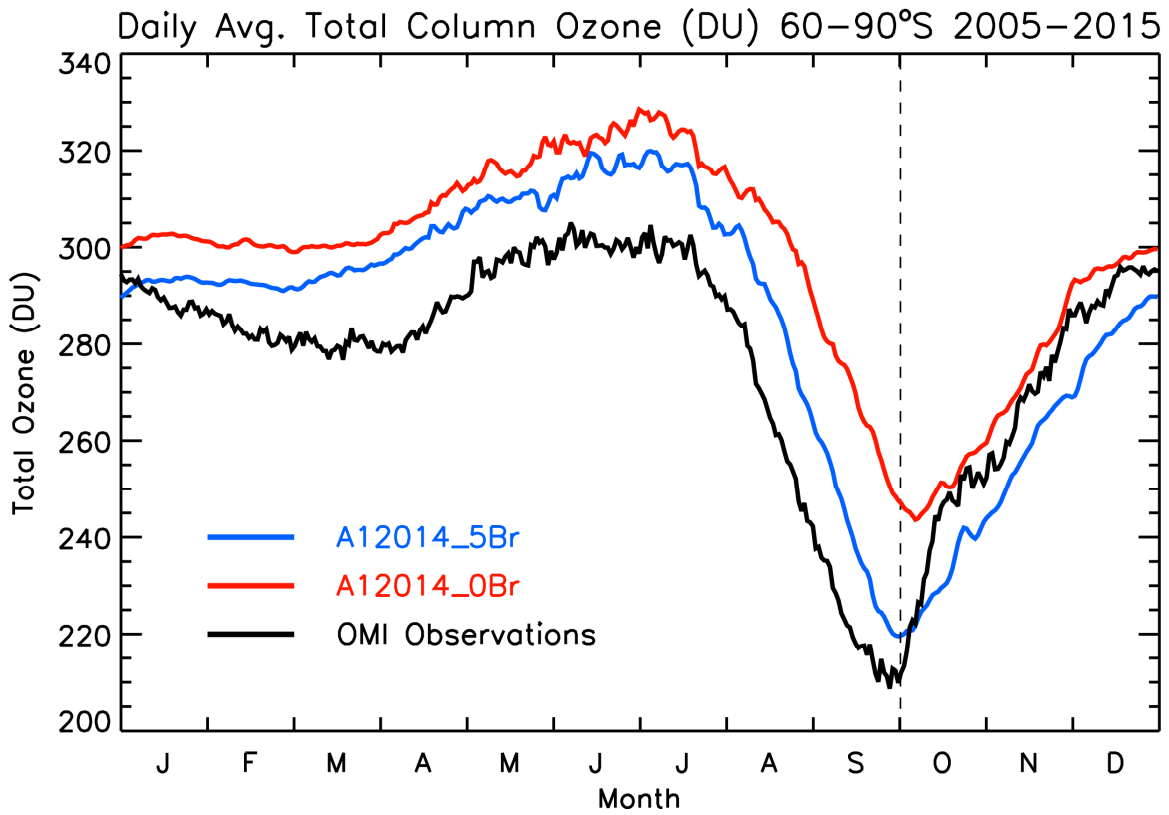
446 World Meteorological Organization (2014), Scientific assessment of ozone  
447 depletion: 2014, Global Ozone Research and Monitoring Project-Report No. 55,  
448 416 pp., Geneva, Switzerland.

449 Yang, X., N. L. Abraham, A. T. Archibald, P. Braesicke, J. Keeble, P. J. Telford, N. J.  
450 Warwick, and J. A. Pyle (2014), How sensitive is the recovery of stratospheric  
451 ozone to changes in concentrations of very short-lived bromocarbons?, *Atmos.*  
452 *Chem. Phys.*, 14, 10,431–10,438.

453

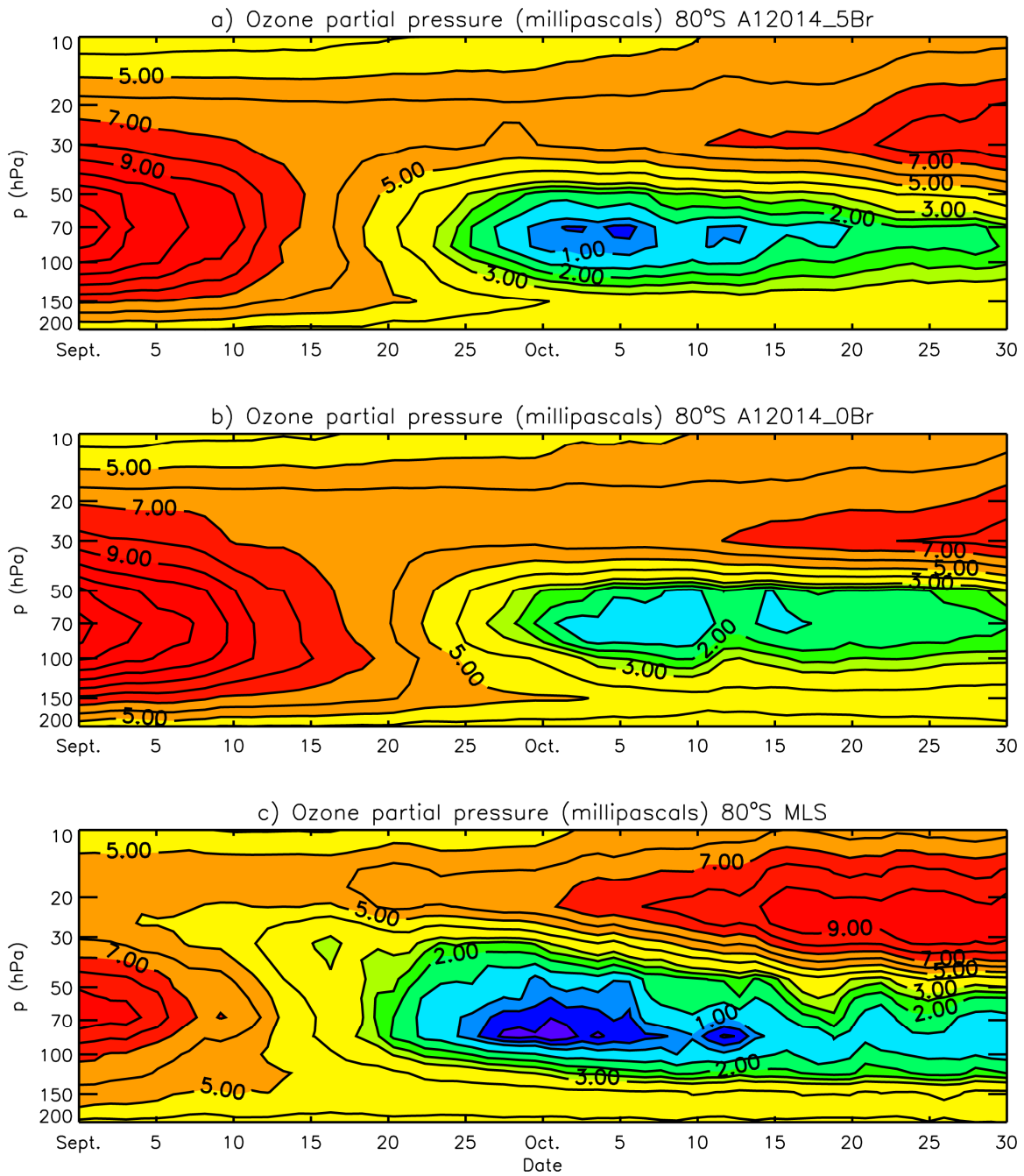
454

455 **Figures**  
456  
457  
458



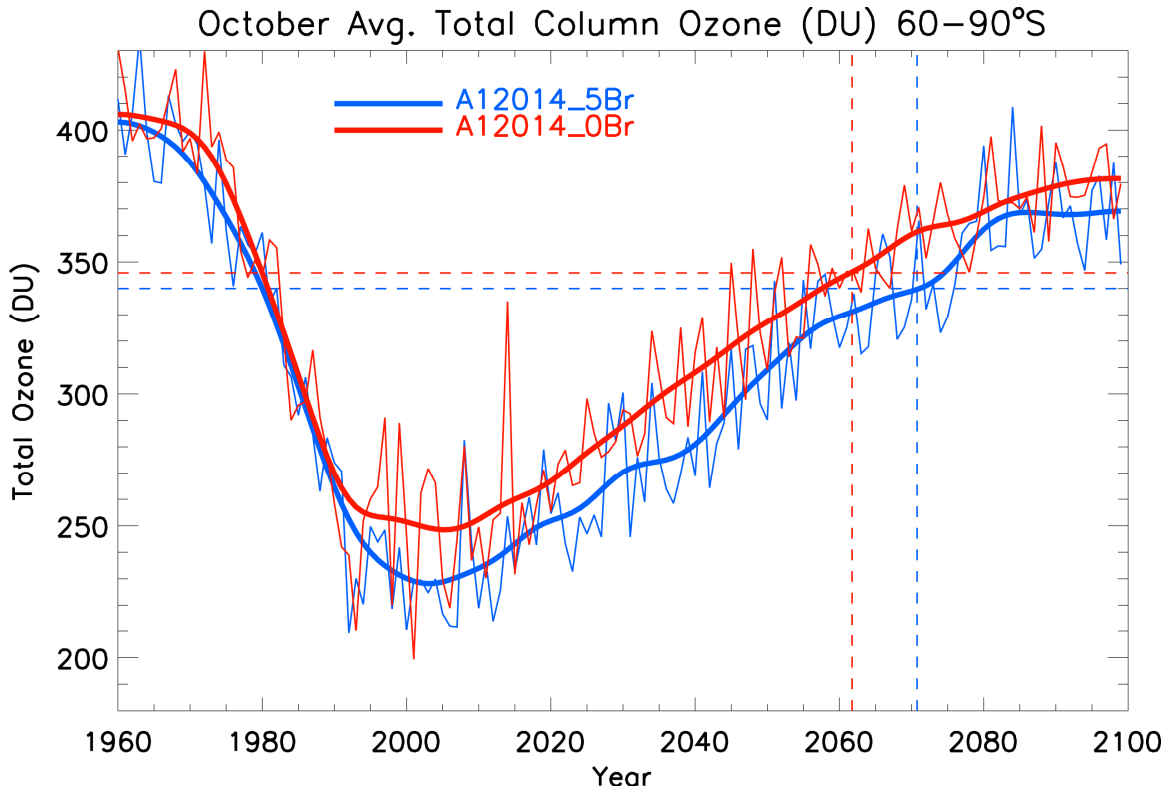
459  
460  
461  
462  
463  
464  
465

Figure 1. The daily average total column ozone (DU) between 60-90°S for 2005-2015. The blue curve shows the A12014\_5Br simulation, the red curve is the A12014\_0Br simulation, and the black curve is the OMI observation. A dashed black line shows 1 October.



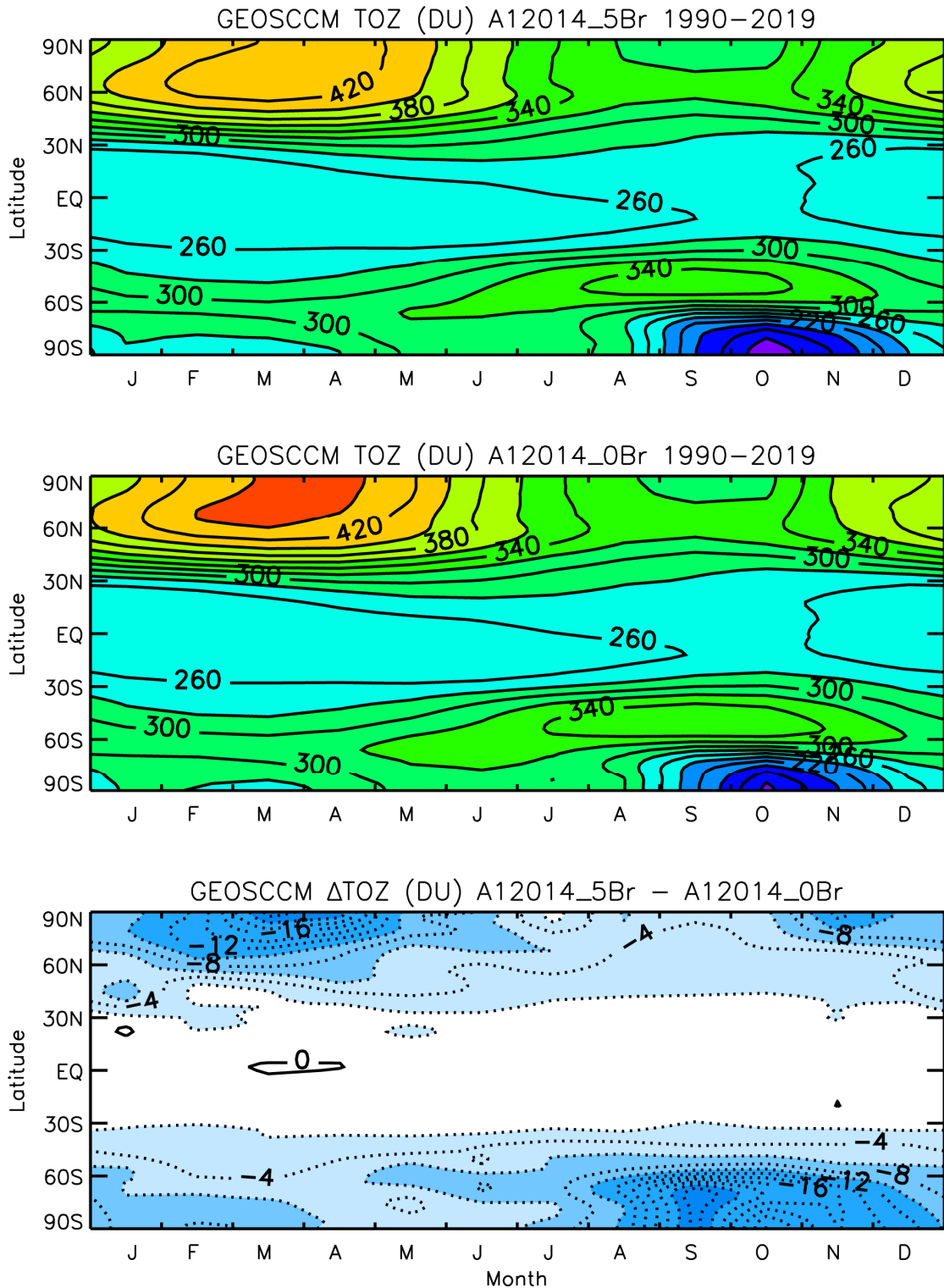
466  
 467  
 468  
 469  
 470  
 471  
 472

Figure 2. Daily ozone partial pressure (millipascals) at 80°S for a) A12014\_5Br, b) A12014\_0Br, and c) MLS measurements from 1 September to 30 October averaged over 2005-2009. The contour interval is 0.25 between 0 and 1 and 0.5 between 1 and 3 and 1 above 3.



473  
 474  
 475  
 476  
 477  
 478  
 479  
 480  
 481  
 482  
 483

Figure 3. The October average total column ozone (DU) between 60-90°S from 1960 to 2099. The blue curves show the individual year values (thin) and low pass filtered values (thick) for the simulation with an extra 5 ppt of bromine. The red curves show the individual year values (thin) and low pass filtered values (thick) for the simulation without a representation of bromine from VLS. The vertical dashed red and black lines represent the return to 1980 levels using the smoothed curves without the extra Br and the simulation with the extra Br.



484  
 485  
 486  
 487  
 488  
 489

Figure 4. The latitude by month total column ozone (DU) for the A12014\_5Br (top panel) and A12014\_0Br (middle panel) simulations average over 1990-2019. The bottom panel shows the difference in total column ozone (DU) between the two simulations.